Proceedings of the 17th World Congress
The International Federation of Automatic Control
Seoul, Korea, July 6-11, 2008

Optimal Selection of Control Inputs for Diesel Engines

Daniel Alberer, Markus Hirsch, Luigi del Re

Institute for Design and Control of Mechatronical Systems
Johannes Kepler University Linz, Austria

e-mails: {daniel.alberer, markus.hirsch, luigi.delre}@jku.at

Abstract: Diesel engine NO_x and *PM* emissions are characterized by a combination of many system inputs. Since more than one combination of inputs leads to the same output and the high number of degrees of freedom, it is an ill-posed problem to determine the optimal input combination. In this paper the introduction of a two dimensional coordinate system is addressed, with the target of a separate and independent control of NO_x and *PM*. Finally, a validation on testbench data is presented.

1. INTRODUCTION

In order to cope with the increasing and conflicting demands in terms of pollution abatement, drivability and economy, modern engines have become complex systems with many inputs and thus a high number of degrees of freedom, like variable geometry turbocharger, exhaust gas recirculation, variable swirl, multiple injections, variable injection pressure etc. However, engines are strongly interconnected systems and most control inputs affect several target quantities at the same time, in particular emissions, so that an emission oriented engine control is mostly an ill-conditioned problem.

Governmental restrictions cause passenger car manufacturers to focus on emissions, whereas the two possible measures are raw emission control or the use of after-treatment systems. In contrast to Otto engines the 3-way catalyst does not work for Diesel engines and after-treatment systems have not yet reached their maturity and efficiency (Pfahl, *et al.*, 2003). Thus, there is substantial interest in controlling the engine raw emissions, in particular the nitric oxides (NO_x) and the particulate matter (*PM*), generated during the combustion (see *e.g.* (Heywood, 1988)).

Unfortunately, almost all engine control inputs have an opposite effect on *PM* and on NO_x, *i.e.* by reducing one quantity the other one is increased (see Figure 3). Many works have been published that investigate the so called NO_x-*PM* tradeoff, see *e.g.* (Tow, *et al.*, 1994), (Richards, *et al.*, 2001), or (Hountalas, *et al.*, 2003).

Figure 1 shows the measured NO_x-*PM* tradeoff of a Euro 4 common rail Diesel engine for constant speed and main injection quantity. Out of this figure one can determine a Pareto optimum. Obviously, the production standard measurement point is not on this line. This is due to the fact, that emissions need not be minimized, but to be kept cumulatively under a limit and thus other targets like drivability, consumption or combustion noise can be improved.

In practice, the ill-condition and the availability of many inputs lead to strong challenges for the control design. To simplify the task, usually the problem is restated in terms of some intermediate variables, typically boost pressure and fresh air mass, since these two quantities can easily be used for a feedback control, see e.g. (Ammann, *et al.*, 2003).

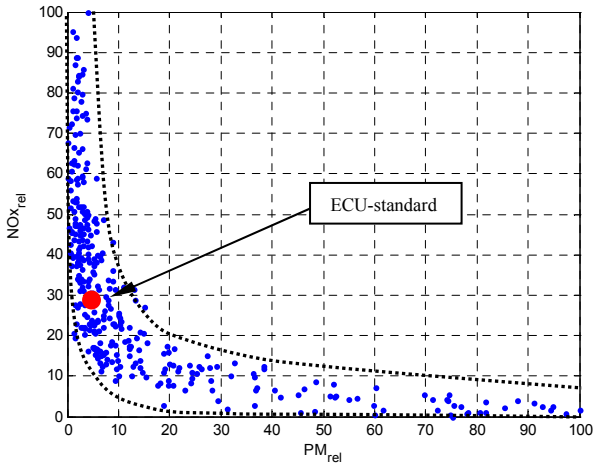

Figure 1: NO_x-*PM* tradeoff (2000rpm, 0.7MPa *BMEP*)

However, other quantities have been tested, so (Nakayama, *et al.*, 2003) have investigated the transient NO_x peaks and their reduction by oxygen intake concentration (OIC) control, (Langthaler and del Re, 2007) apply model predictive control for OIC control, or (Darlington, *et al.*, 2006) use simple first principle models to reduce transient emission peaks. In (Knafl, *et al.*, 2005) an optimization of combustion parameters is performed by a polynomial map approximation of the input/output relations, or (Boulouchos, *et al.*, 2000) optimize the injection pattern.

This paper is somehow a generalization of these approaches, but starts from a different point of view. Instead of looking for an intermediate quantity to be set, we look for combinations of inputs directly correlated to the main quantities to be controlled. The main idea is quite simple: this

combination can be treated as a single input associated to a single output quantity, allowing a steady state system decoupling and a much simpler problem statement. While every control system, even the standard heuristic approaches conventionally used, do solve the same problem in some indirect form, this decoupling proves extremely useful from two points of view: on one side, it allows a systematic choice of the NO_x-PM tradeoff, on the other side it defines the relation between control inputs to be observed during transients to avoid emission peaks.

2. PROBLEM STATEMENT

2.1 The Plant

In Figure 2 the layout of a standard passenger car Diesel engine is sketched. It can be separated into two main parts, on one hand the airpath with the turbocharger, exhaust gas recirculation (EGR) and swirl actuation and on the other hand the injection path with the common rail and the injectors.

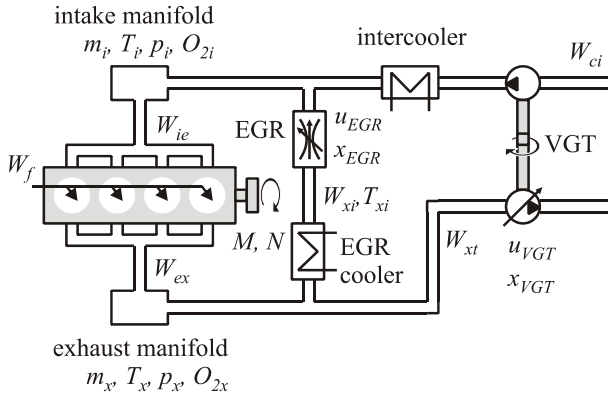

Figure 2: Diesel engine layout

2.2 System Setup

The analyses were done on an AVL testbed and a 2 liter BMW EU4 common rail Diesel engine. In this paper we analyze the emissions at a constant operating point of the engine, defined by fixed values of main injection quantity and engine speed (which are 2000rpm and equals a load of approximately 0.7MPa *BMEP*). The variable selection could be done with standard statistical approaches, e.g. (Guyon and Elisseeff, 2003), but in this work the same control inputs and measurements were used as available and used in the standard production version. As far as the injection path is concerned, the system state is defined by the common rail pressure, the injected fuel quantities and the injection timing. Due to the fact, that the turbocharger guide vane position. the EGR valve opening and the total injection amount determine the air to fuel ratio and the intake oxygen concentration, these latter quantities were used directly for identification instead of the actuator positions. Of course, the swirl actuation needs to be included too. In summary, the following quantities were used for identification:

- Intake oxygen concentration O_2
- Air to fuel ratio λ
- Swirl actuation Sa (swirl on/off only)
- Injection
  - Angle of main injection φ_{MI}
  - Quantity q_{PI} and timing ti_{PI} of pre-injection
- Common rail pressure

For numerical stability both the system inputs and the considered target channels were scaled to a range of [0...100]. The whole analysis is based on steady state data. Thus, after a setpoint change the system had to settle before data acquisition was done.

2.3 Objective

All system inputs influence both NO_x and PM. In Figure 3 the impacts of four different inputs can be seen, with different sensitivities and also different directions.

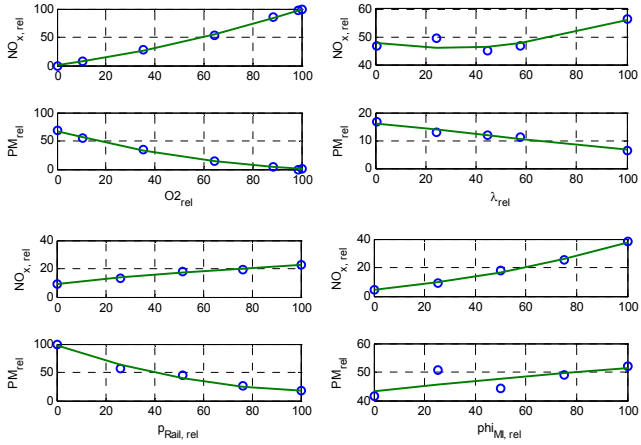

Figure 3: Influences of several inputs on NO_x/PM emissions

Here the target is to find new coordinates as a superposition of the several inputs, which results in an orthogonalized two dimensional coordinate system (Figure 4 depicts a sketch of this target.). Afterwards, this coordinates can be used for a separate and independent control of the emissions, e.g. NO_x is kept constant while PM is changed arbitrarily within the physical boundaries of the system.

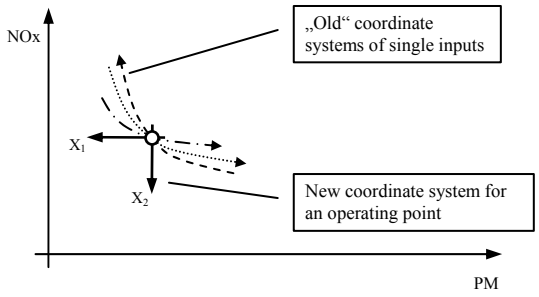

Figure 4: Single input sensitivities and new coordinate system for an operating point

The target of an orthogonal coordinate system can be expressed as an optimization problem. The sensitivity of the

main direction is maximized, whereas the cross sensitivity is minimized. Equation (1) represents this optimization. For coordinate one the sensitivity of *PM* to the inputs is maximized, whereas the absolute sensitivity of NO_x to these inputs is minimized, and vice versa for coordinate two.

$$X_1 = f_1(x_i)\big|_{i=1\ldots n} = \arg(\max \sum_N \frac{\partial PM}{\partial X_1} \,\&\, \min \left\| \sum_N \frac{\partial NOx}{\partial X_1} \right\|) \qquad (1)$$
$$X_2 = f_2(x_i)\big|_{i=1\ldots n} = \arg(\max \sum_N \frac{\partial NOx}{\partial X_2} \,\&\, \min \left\| \sum_N \frac{\partial PM}{\partial X_2} \right\|)$$

where X_1, X_2 denote the orthogonal coordinates. The functions f_1, f_2 represent a tensor in the coordinates of the inputs u, N is the number of measurements and n the number of coefficients in f. In the following it is shown how these coordinates can be found directly without the use of optimization techniques.

2.4 Design

Firstly, a steady state measurement characterized by constant engine speed and *BMEP* was taken, whereas the inputs were changed randomly at discrete time instants and steady state data was recorded. Hence, 330 data points in the NO_x/*PM* plane were detected. As a basis the standard ECU working point was measured, too. In particular in case of low air fuel ratios and thus high *PM* values, the combustion efficiency decreased significantly with the result of a lower *BMEP*. The focus of the coordinate system should be on the closer region of the standard ECU setpoint. Therefore, all measurement data within a specific distance to this operating point and with normal *BMEP* was collected, and afterwards a first order linearization was identified (see Figure 5).

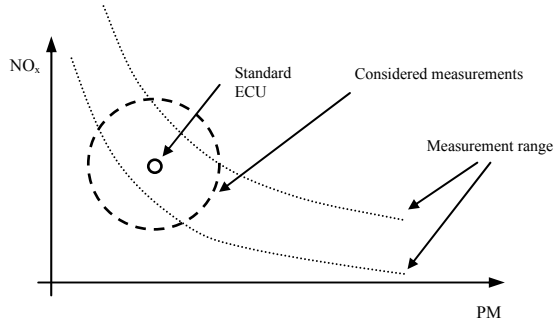

Figure 5: Data collection for first order approximation

To explain the used approach we start with a general description. Based on a Taylor series approximation of an arbitrary nonlinear function f at a point x

$$f(x+\Delta x) = f(x) + \frac{\partial f}{\partial x}\Delta x + \frac{\partial^2 f}{\partial x^2}\frac{(\Delta x)^2}{2!} + \frac{\partial^3 f}{\partial x^3}\frac{(\Delta x)^3}{3!} + \ldots = f(x) + \sum_{n=1}^{\infty} \frac{\partial^n f}{\partial x^n}\frac{(\Delta x)^n}{n!} \qquad (2)$$

one can reform

$$f(x+\Delta x) - f(x) = \Delta f(x) = \sum_{n=1}^{\infty} \frac{\partial^n f}{\partial x^n}\frac{(\Delta x)^n}{n!}. \qquad (3)$$

Truncating after the first term we get

$$\Delta f(x) = \frac{\partial f}{\partial x}\Delta x + O((\Delta x)^2). \qquad (4)$$

In (4) the in-/output difference relation with the sensitivity $\frac{\partial f}{\partial x}$ is described. Transferring (4) to the emission modeling formulation we get the first order linearization

$$\Delta PM = \underbrace{\sum_{i=1}^{n_u} x_{1,i} \cdot \Delta u_i}_{\Delta PM^*} + e_1$$
$$\Delta NOx = \underbrace{\sum_{i=1}^{n_u} x_{2,i} \cdot \Delta u_i}_{\Delta NOx^*} + e_2 \qquad (5)$$

with the sensitivities $x_{1,i}$, $x_{2,i}$. Obviously, a higher order description would be possible and was tested, but found to induce a tremendous increase of parameters without a significant improvement of the result. The sensitivities are determined by a standard least squares minimization (see e.g. (Ljung, 1999)) of the modeling errors e_1, e_2, *i.e.* the linearization of a nonlinear function is identified directly.

$$\theta = (\phi^T \cdot \phi)^{-1} \cdot \phi^T \cdot Y \qquad (6)$$

Equations (5) give absolute descriptions of the emission gradients, thus by moving into the direction of $\Delta PM^*/\Delta NO_x^*$ the target of maximization of the sensitivity to the main component is fulfilled. Furthermore, the minimization of the cross sensitivities leads to the desired coordinates. The coordinates X_1, X_2 can finally be determined by the equation of ΔPM^* at constant ΔNO_x^* and vice versa.

$$X_1 = \Delta PM^*\big|_{\Delta NOx^* = const.}, \quad X_2 = \Delta NOx^*\big|_{\Delta PM^* = const.} \qquad (7)$$

With the relations (5) two high dimensional planes are described. Setting one equation to zero fixes one plane. Finally, the solution is the intersection with the second plane.

3. RESULTS

3.1 Identification

All data within a specified distance around the standard ECU measurement point was used to identify first order approximations of the target functions (see Figure 6). In Figure 7 the identification results are shown (Every data point represents a single steady state measurement). The relative quadratic fit of the identification is 54.4% for *PM* and 74.4% for NO_x and in validation 57.0% for *PM* and 79.1% for NO_x.

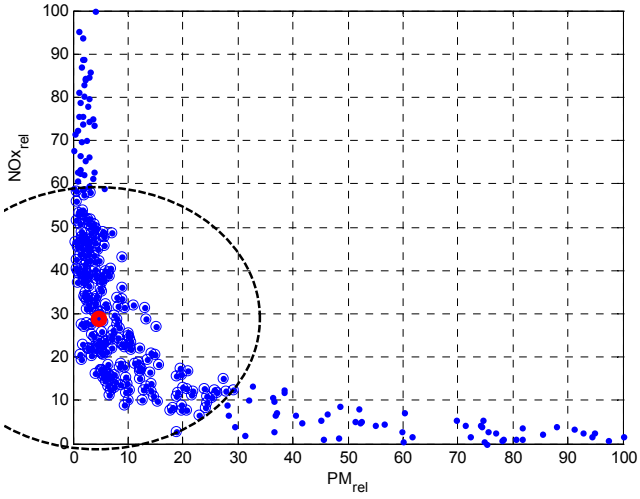

Figure 6: Identification data (radius 30%)

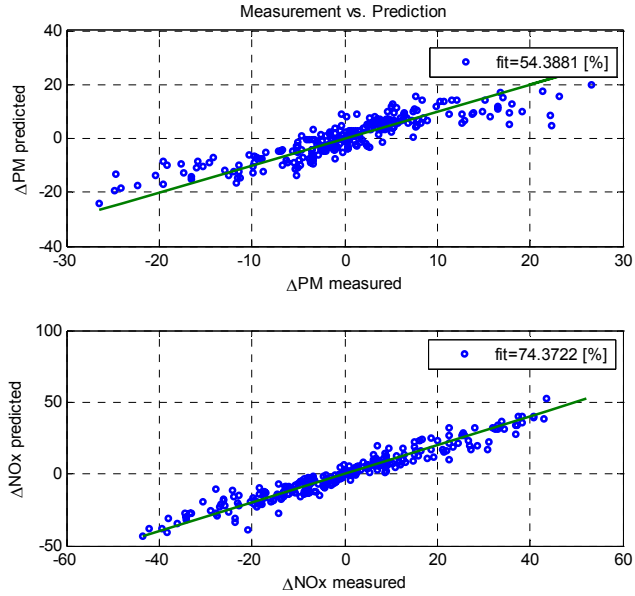

Figure 7: Identification of $\Delta PM/\Delta NO_x$ emissions

In Figure 8 validation data is presented, whereas this is real extrapolation since the data within a radius from 30%-60% was used for validation. In particular the highly nonlinear behavior of large ΔPM values cannot be captured perfectly. The result for ΔNO_x on the other hand shows a very good extrapolation. The identification result leads to

$$\begin{bmatrix}\Delta PM^* \\ \Delta NO_x^*\end{bmatrix} = c.\begin{bmatrix}-4.73 & -34.48 & 2.69 & -12.30 & -0.38 & -0.65 & -11.50 \\ 8.95 & 105.01 & -6.34 & 11.29 & 16.31 & -0.40 & -14.34\end{bmatrix}.\begin{bmatrix}\Delta Sa \\ \Delta O_2 \\ \Delta q_{PI} \\ \Delta p_{Rail} \\ \Delta \varphi_{MI} \\ \Delta ti_{PI} \\ \Delta \lambda\end{bmatrix} \quad (8)$$

In this case the condition number (relation of maximum to minimum singular value) of the information matrix $(\phi^T \cdot \phi)$ has a reasonable value of 68.5. With respect to the nonlinear nature of the system one has to be careful when concluding based on the linear approximation of (8). However, not all of the parameters seem to have the right sign. Concretely, the negative sensitivity of ΔNO_x^* to $\Delta\lambda$ is not plausible. Here it seems, the reason for this is a too high estimated positive sensitivity to O_2.

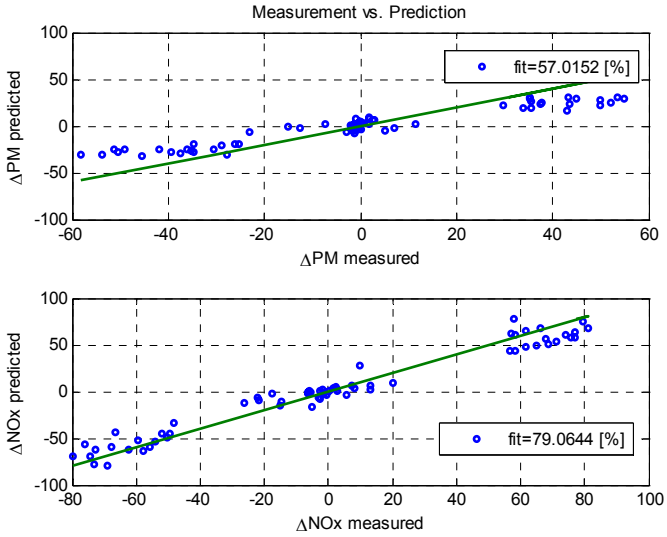

Figure 8: Measurement and prediction of $\Delta PM/\Delta NO_x$ emissions

A more detailed analysis yields to the conclusion that the switching swirl actuation leads to a strong change in the system behavior too. Therefore, a further identification was done with high swirl data only.

$$\begin{bmatrix}\Delta PM^* \\ \Delta NO_x^*\end{bmatrix} = c.\begin{bmatrix}-28.05 & 2.33 & -8.93 & -0.18 & -0.13 & -10.14 \\ 112.14 & -7.55 & 11.46 & 22.30 & 2.61 & 2.38\end{bmatrix}.\begin{bmatrix}\Delta O_2 \\ \Delta q_{PI} \\ \Delta p_{Rail} \\ \Delta \varphi_{MI} \\ \Delta ti_{PI} \\ \Delta \lambda\end{bmatrix} \quad (9)$$

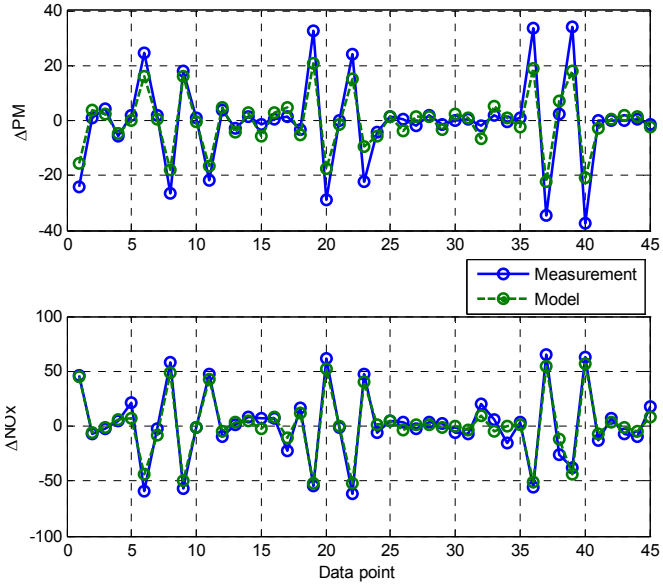

Figure 9: Validation for high swirl data, formulation (9)

The fit-values in identification are 65.1% for *PM* and 78.0% for NO_x and in validation 58.2% for *PM* and 76.5% for NO_x, the condition number is 57.4. Comparing the identified parameters of (8) and (9) one can see, that they have similar values except the sensitivities of ΔNO_x^* *to* Δti_{PI} and $\Delta\lambda$. Finally, the sensitivity coefficients are all in a reasonable range. A validation at extrapolation data is shown in Figure 9.

3.2 Emission control

To validate the formulations of (8) and (9), a steady state compensation was implemented on the testbench, at which either X_1 or X_2 was kept at a constant value, while the other coordinate was altered. Figure 10 depicts a steady validation of the

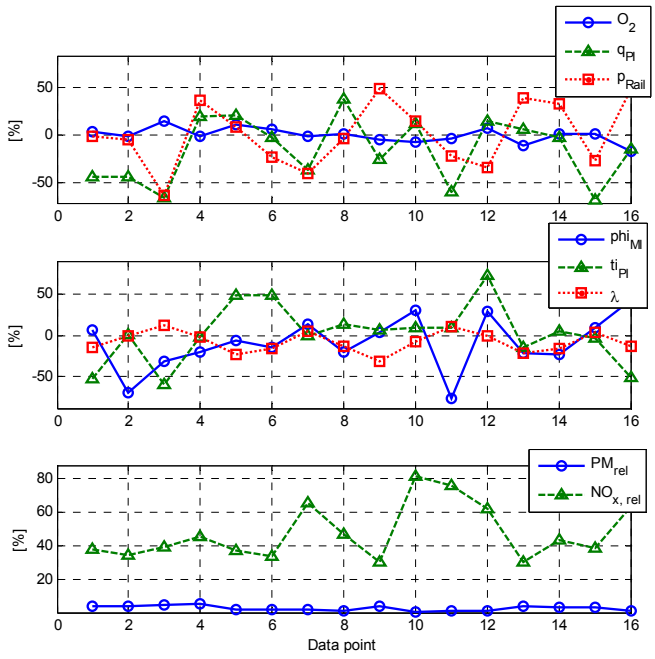

Figure 10: X_1 = const., validation of (9)

high swirl data (9). While *PM* was kept almost constant, the NO_x values changed. In the top part the adjusted input values can be seen - the railpressure was controlled to keep ΔPM zero.

In Figure 11 a dataset with a validation of (8) is presented. By keeping X_2 constant, the switching swirl actuation can be compensated. As a consequence the *PM* values need to be changed. For a comparison during 110-210s the compensation was turned off, which caused large amplitudes of NO_x. In this case the *PM* emissions were not influenced significantly, which mainly is explained by the high air to fuel ratio in this point that makes *PM* less sensitive to swirl.

In the bottom part of Figure 11 one can see the compensation acting on the rail pressure. The dynamical effects during switching cannot be compensated, since the coordinates are only valid for steady state. Figure 12 shows a 3D representation of altering one coordinate by keeping the other one constant. Therefore, the system inputs were manipulated according to (9), i.e. the several inputs were changed such that the first line of (9) was kept at a constant value and the second changed. In other words, altering X_2 nearly has no influence on *PM* emissions, if X_1 is kept constant, i.e. NO_x is proportional to X_2 for constant X_1 ($\Delta NO_x \sim X_2\big|_{X_1=const.}$).

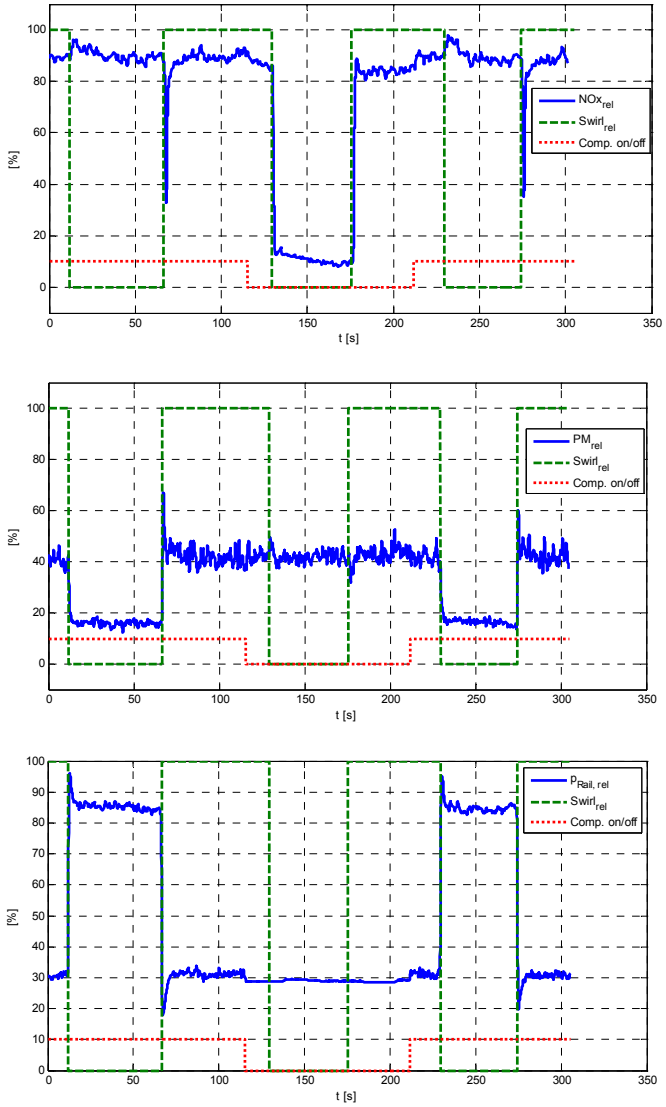

Figure 11: Constant NO_x during swirl switching with and without ($t \approx 110-210\text{s}$) compensation – validation of formulation (8)

4. CONCLUSIONS

The approach presented allows adjusting NO_x and *PM* independently within the physical limits of the engine setup. Of course the absolute limits cannot be overcome, but exploited in a convenient way. The many degrees of freedom are reduced to two coordinates, which can easily be processed in a further use.

In many operating modes a separate control of *PM* and NO_x is desired, *e.g.* during a tip in the peaks need to be kept under a certain limit, or visible smoke must be avoided for any working point. With the presented method, the high dimensional problem is reduced to an order of two.

Therefore, application of different strategies are easily possible, *i.e.* to force constant NO_x during a transient or a constant relation of NO_x and *PM*.

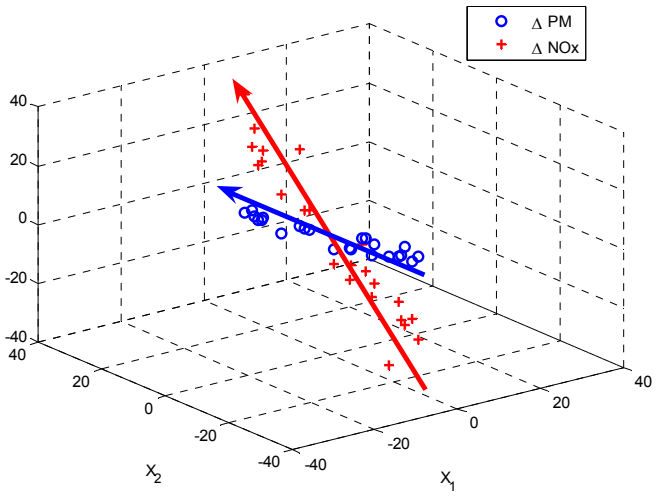

Figure 12: Altering X_2 and keeping X_1 constant leads to constant *PM* and a change in NO_x

Although the optimization of a working point like in (Gschweitl, *et al.*, 2001) or in (Hagena, *et al.*, 2006) is not the objective for this transformation, it can be used for an online optimization, too. However it is not intended to be used for ECU calibration, but as mentioned before for a later online control.

In Figure 11 an interesting effect can be seen. The response immediately after switching is nearly the same with or without compensation. Only when the system begins to settle, the target value of constant NO_x is approached in case of compensation. Obviously, the compensation is only valid for steady state or if infinite fast actuators would be available. This dynamical response during switching gives a scope for further dynamical modeling. Possibly a simple structure with the here presented steady state description and linear dynamics could be able to capture the whole emission behavior. Based on this, optimal control techniques could be applied to control NO_x and *PM*, even linear methods.

A crucial issue for the next steps will be the combination of several local coordinate systems. Besides switching, a LPV structure is also likely to be considered. A further aspect of the sensitivity analysis associated with this method is the possibility to determine the relative importance of the actuators and modify accordingly their layout.

5. REFERENCES

Ammann, M., N. P. Fekete, L. Guzzella and A. H. Glattfelder (2003). Model-based Control of the VGT and EGR in a Turbocharged Common-Rail Diesel Engine: Theory and Passenger Car Implementation. In: *2003 SAE World Congress*, Detroit, Michigan.

Boulouchos, K., H. Stebler, R. Schubiger, M. K. Eberle and T. Lutz (2000). Optimierung von Arbeits- und Brennverfahren für größere Dieselmotoren mit Common-Rail-Einspritzung (2). In: *MTZ*,

Darlington, A., K. Glover and N. Collings (2006). A simple diesel engine air-path model to predict the cylinder charge during transients: Strategies for reducing transient emissions spikes. In: *SAE Powertrain & Fluid Systems Conference and Exhibition*. Toronto, Ontario, Canada.

Gschweitl, K., H. Pfluegl, T. Fortuna and R. Leithgoeb (2001). Steigerung der Effizienz in der modellbasierten Motorenapplikation durch die neue CAMEO Online DoE-Toolbox. *ATZ,* **7,**

Guyon, I. and A. Elisseeff (2003). An Introduction to Variable and Feature Selection. *Journal of Machine Learning Research,* **3,** 1157-1182.

Hagena, J. R., Z. S. Filipi and D. N. Assanis (2006). Transient Diesel Emissions: Analysis of Engine Operation During a Tip-In. In: *2006 SAE World Congress*, Detroit, Michigan.

Heywood, J. B. (1988). *Internal Combustion Engine Fundamentals*, New York.

Hountalas, D. T., D. A. Kouremenos, K. B. Binder, V. Schwarz and G. C. Mavropoulos (2003). Effect of Injection Pressure on the Performance and Exhaust Emissions of a Heavy Duty DI Diesel Engine. In: *2003 SAE World Congress*, Detroit.

Knafl, A., J. R. Hagena, Z. S. Filipi and D. N. Assanis (2005). Dual-Use Engine Calibration: Leveraging Modern Technologies to Improve Performance - Emissions Tradeoff. In: *2005 SAE World Congress*, Detroit, Michigan.

Langthaler, P. and L. del Re (2007). Fast Predictive Oxygen Charge Control of a Diesel Engine. In: *2007 American Control Conference*, New York City, USA.

Ljung, L. (1999). *System Identification - Theory For the User*, PTR Prentice Hall, Upper Saddle River, N.J.

Nakayama, S., T. Fukuma, A. Matsunaga, T. Miyake and T. Wakimoto (2003). A New Dynamic Combustion Control Method Based on Charge Oxygen Concentration for Diesel Engines. In: *SAE*, SAE International,

Pfahl, U., W. Hirtler and T. Cartus (2003). Passenger Car Investigations of NOx-Adsorber and DPF Combination to Fulfill Future Diesel Emission Limits In: *SAE World Congress*, Detroit, Michigan.

Richards, K. J., M. N. Subramaniam, R. D. Reitz, M.-C. Lai, N. A. Henein and P. C. Miles (2001). Modeling the Effects of EGR and Injection Pressure on Emissions in a High-Speed Direct-Injection Diesel Engine. In: *SAE 2001 World Congress*, Detroit.

Tow, T. C., D. A. Pierpont and R. D. Reitz (1994). Reducing Particulate and NOx Emissions by Using Multiple Injections in a Heavy Duty D.I. Diesel Engine. In: *SAE World Congress*, Detroit.